Influence of fluid flow characteristics and heat transfer in a tube heat exchanger using H-shape inserts with circular ring

DOI : 10.36909/jer.ICCEMME.15861

Satyendra Singh*, Tarun Joshi**, Himanshi Kharkwal**

**Professor, Department of Mechanical Engineering,B.T.Kumaon Institute of Technology, Dwarahat Almora, India*
***M.Tech. Scholar, Department of Mechanical Engineering,B.T.Kumaon Institute of Technology, Dwarahat Almora, India*
Corresponding author email: ssinghiitd@gmail.com

ABSTRACT

The heat transfer and fluid flow characteristics in a tube heat exchanger using H-shape inserts with circular ring (CRWHS) has been done by computationally and experimentally. In this investigation parameters like ratio of the diameters and pitches are considered. The value of diameter and pitch ratios are (DR=0.8, 0.9), (PR=3, 4) respectively. The main section in which investigation was done is 1.5m long and the hydraulic diameter of the tube is 68.1mm. 1000 W/m^2 heat flux was provided in the main section. Heat flux was constant throughout the investigation. Air is used as a working medium in which 6000 to 21000 Reynolds number was used for the investigation. The observation revealed that the increment in heat transfer rate is 4.56 times as compare to smooth tube for the circular ring with H-shape inserts. In case of DR=0.8 and PR=3, maximum thermal performance factor was obtain which is 3.24. In GIT the deviation in Nusselt number & friction factor is limited to ±0.4% & ±0.1% respectively. CFD analysis result comparisons with experimental one are presented in which the maximum deviations for thermal performance factor are limited to ±3.6%.

Keywords: Tube heat exchanger, Nusselt number, H-shape inserts, Friction factor

INTRODUCTION

Heat exchanger is a tool which is exchanger energy from one source to another source or from a heated wall to single fluid. Heat exchangers are required in thermal power plants, industries, HAVC applications, refrigeration & air conditioning, chillers etc. (Datt et al., 2018) investigate square wing with solid ring and twisted tape inserts to observed the behavior of heat transfer rate and friction factor in the tube heat exchanger as a result they found 2.74 maximum thermal performance factor and increment in heat transfer is 5.66 times over smooth tube. (Kumar et al., 2016) investigate hollow circular disc of solid inserts experimentally and circular perforated ring inserts within circular tube and found a thermal performance increased by 1.4 times in case of former insert and 1.47 times as compare to smooth tube values in case of latter insert. (Kongkaitpaiboon et al., 2010) studied influence of circular ring tabulators for a tube heat exchanger experimentally which resulted for smaller diameter and pitch ratios the increment in heat transfer is 195% as compare to plain tube. (Eiamsa-ard et al., 2013) experimentally perused that for turbulent flow regime in circular rings with twisted tape insert within tube heat exchanger and observed that thermal performance increased by 1.42 times compare to smooth tube. (Akcayoglu et al., 2011) in his experimental investigation done in ducts with half delta wings with double rows pair having arrangement of common flow up and down configuration effect of delta-wing double sided insert with different axes was studies by (Eiamsa-ard and Promvonge, 2011). They varied wing arrangement, wing-width ratios and wing pitch ratios. Results reveled that forward wing arrangement and alternate axes gives better heat transfer augmentation than the double-sided delta wings. Delta winglets with different arrangements were investigated by (Aliabadi et al., 2015). They studied fourteen vortex-generator insert with longitudinal and forward arrangement of delta winglets. (Zhu and Chen et al., 2015) in their numerical investigation carried the work on twisted tapes. They used different twisted tapes like single, double and triple and found that all of the three types of insert can increase the rate of heat transfer ability to 1.8 to 4.5 times over a plain tube. While (Vashistha et al., 2016) studied different twisted tape inserts single, twin and four in which they varied the twist ratio by experimentally.

Further CFD simulation of in-tube twisted tape was done by (Alzahrani and Usman, 2019). They came forward with certain conclusion that, to enhance heat transfer rate, pressure drop for the tube heat exchanger having twisted tapes inserts is always higher over the plain tubes and also conclude that small twist ratio gives better results to increment of heat transfer and width of tape also influenced heat transfer and friction. (Hong et al., 2019) presented the effect of Reynolds number, pitch length, rib height and tape number on friction factor, Nusselt number and TPF. From their numerical investigation they found that these inserts when placed inside the tube makes the distribution in which the creation of thermal resistance and turbulence intensity will be acting more which trend to higher heat transfer rate. (Gholamalizadeh et al., 2019) in their numerical studies investigated about thermal energy transfer and pressure drop intensification due to coiled wire inserts of different cross sectional form. Further perforated discontinuous helix turbulators studied by (Sheikholeslami et al., 2016), resulted that the rise in open area ratio and pitch ratio the nusselt number and friction factor reduces. (Kongkaitpaiboon et al., 2010) started the work on solid hollow circular ring in which they varied the geometric parameters like diameter and pitch ratios and revealed that, smallest pitch and diameter ratios gives higher rate of heat transfer. Similarly (Kumar et al., 2016) used circular rings and varied different diameter ratio with pitch ratio and found maximum enhancement of 1.39 at diameter ratio 0.8 and pitch ratio of 1. In their further investigation, they used perforation in circular rings in which they used different perforation index where they found at perforation index of 24 % and diameter ratio of 0.8, TPF enhances 1.47 times of plain tube. (Singh et al., 2019) used circular rings with rectangular winglets for tube exchanger by experimentally where they varied blockage ratio, attack angle and pitch ratio and found TPF enhances 1.95 times over the smooth tube. (Zong et al., 2019) in his numerical investigation finds the nature of 3-Dimensional turbulent flow by inserting a hollow cross disk. Similarly metal wire net in circular ring inserts studied by (Bartwal et al., 2018), revealed that for smaller pitch ratio the Nusselt number increases with increment of the wire net grades. Finite element based model on rectangular boxes were done by (Hossain et al., 2017). They have used rectangular boxes of 5 mm thickness placed horizontally and vertically in the direction of fluid flow. In their investigation they varied the number of inserts. Like the fluid domain was tested with- no inserts two, four, six, eight and ten inserts. The results showed that fluid domain with 4 inserts gives maximum outlet temperature. The literature survey showed that in order to increase the effectiveness of heat exchanger surface disturbances along with core disturbance plays an important role. Therefore such inserts should be introduced which increases heat transfer with comparatively less enhancement in friction factor and thereby increasing thermal performance factor.

METHODOLOGY

For enhancement of the heat transfer we can understand the mechanism of circular heat exchanger with circular ring with H-shape inserts (CRWHS), for experimental analysis the investigation setup is shown in figs. 1 and 2. For analysis test section is 1.5m in length where 1000 w/m^2 constant heat flux density is provided over the tube wall. Reynolds number varied over 6000 to 21000. In analysis of the computational domain of fluid flow, the flow domain is divided into the sub parts these sub parts are known as cells. For these cells the governing equation are solved. The meshing of the test section & design is done using ANSYS ICEM facility, a noval cut-cell method of assembly meshing is applied and proximity & curvature sizing functions are used for meshing of fluid domain. This process is divides the test section into smaller volumetric elements of desired minimum & maximum size. Geometrical parameters like diameter ratio (DR) and pitch ratio (PR) used different of the experimental work for the inserts. In which, varying the different combinations of the diameter and pitch ratios.

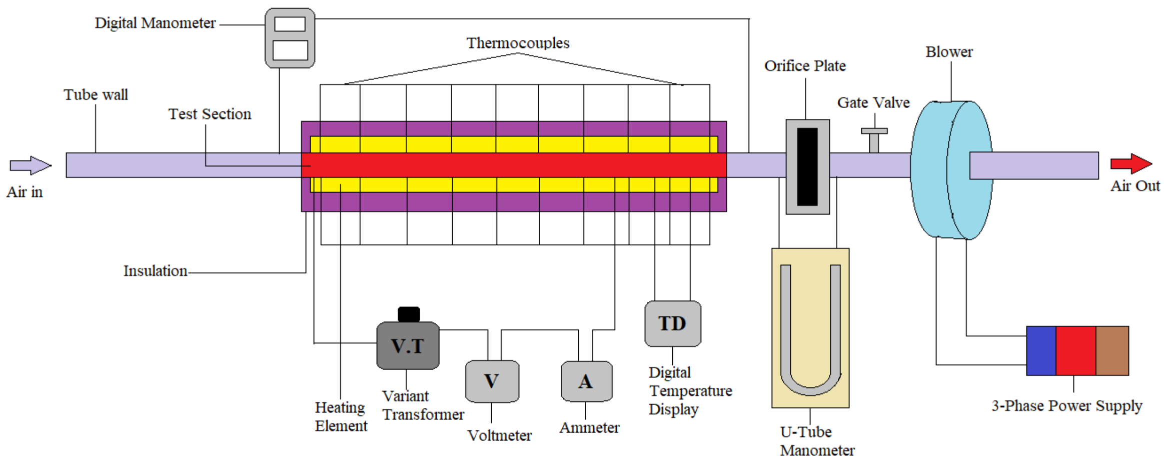

Figure 1 Schematic diagram of experimental setup

Figure 2 Photographic view of experimental setup

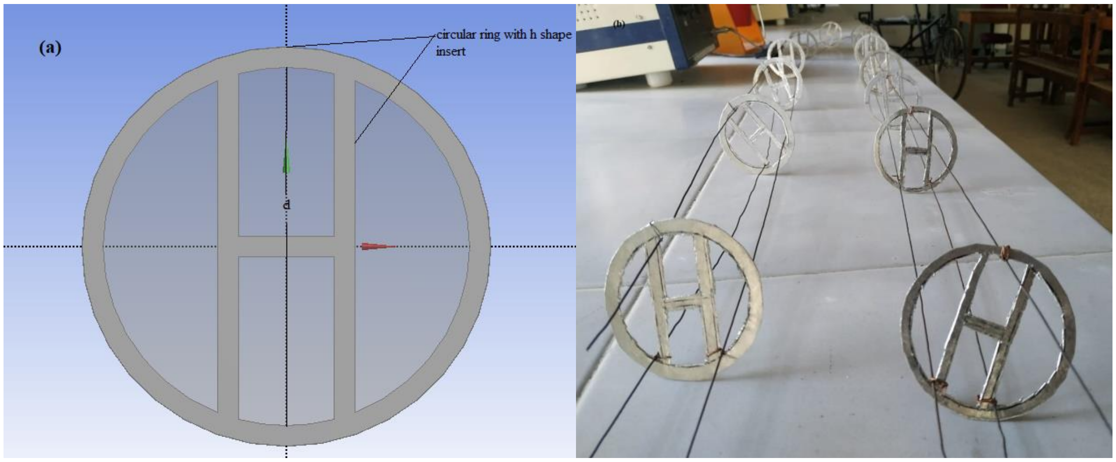

Figure 3 (a) Schematic representations and (b) Pictorial representations of CRWHS insert

MATHEMATICAL FORMULATION

Certain assumptions were considered, for averting minor losses, for the steady-state condition

The energy balance equation is:

$$Q_{air} = Q_{conv.} \tag{1}$$

By equation (1), we can find the average heat transfer coefficient (h), which is:

$$\dot{m}C_p(T_o - T_i) = hA(T_{wm} - T_{fm}) \tag{2}$$

Where T_w and T_{fm} are:

$$T_{wm} = \frac{\sum_{i=1}^{20} Twi}{20} \tag{3}$$

Here T_{wi}= temperature at i^{th} thermocouple

$$T_{fm} = (T_o + T_i)/ 2 \tag{4}$$

$$h = \dot{m}C_p(T_o - T_i) = A(T_{wm} - T_{fm}) \tag{5}$$

For finding the performance, nusselt number and friction factor are evaluated.

$$Nu = \frac{hd}{k} \tag{6}$$

$$f = \frac{\Delta P}{\{(L/D)(\rho V^2/2)\}} \tag{7}$$

To calculate performance of tube heat exchanger we can calculate the TPF by the formula given by (Webb & Kim, 2005).

$$TPF = \frac{(Nu/Nu_s)}{(f/f_s)^{1/3}} \tag{8}$$

By using Blasius and Dittus-Boelter equations we calculate Nu_s and f_s

$$Nu_s = 0.023\, Re^{0.8} Pr^{0.4} \tag{9}$$

$$f_s = 0.316\, Re^{-0.25} \tag{10}$$

RESULTS AND DISCUSSION

The variation of circular ring with H-shape (CRWHS) inserts in a single tube heat exchanger are shown in figures 4, 5and 6 respectively. The fluid behavior inside the tube changes after inserting the CRWHS inserts. In high range of Reynolds number that mean high velocity gives heavy mixing of the fluid due to the inserts hence maximum Nusselt number (*Nu)* is found. However, increasing velocity causes the rise in the friction factor (*f*). Increase in diameter ratio results reduces the contact area of the surface of fluid which reduces the disturbances of the surface and as the result of these decrease both *f* and *Nu*. Decreasing contact area of the surface leads to reduce the intermixing capacity of fluid particles and therefore *Nu* decrease. At *Re* = 6000 maximum heat transfer rate occurs. For CRWHS *Nu* gets increased up to 4.56 times with DR=0.8 and PR=3 at *Re* = 6000. While at DR=0.9 and PR=3 the *f* is minimum 3.13 times for the smooth tube at *Re* = 6000. For CRWHS at *Re* = 6000, DR=0.8 and PR=3 the maximum TPF 3.24 is obtained. Increase in pitch ratio decreased the turbulence intensity as a result decreases the friction factor and Nusselt Number.

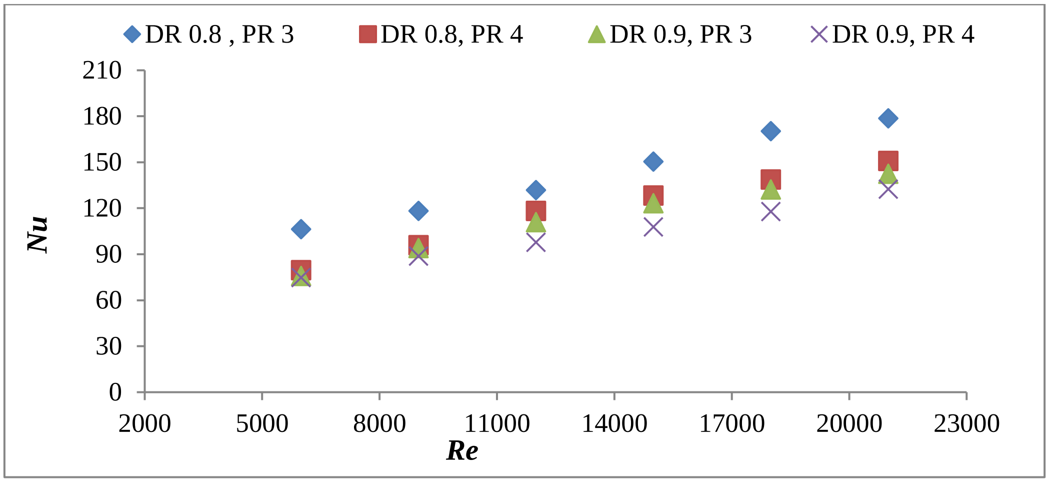

Figure 4 Effect of *Nu* with *Re* for CRWHS

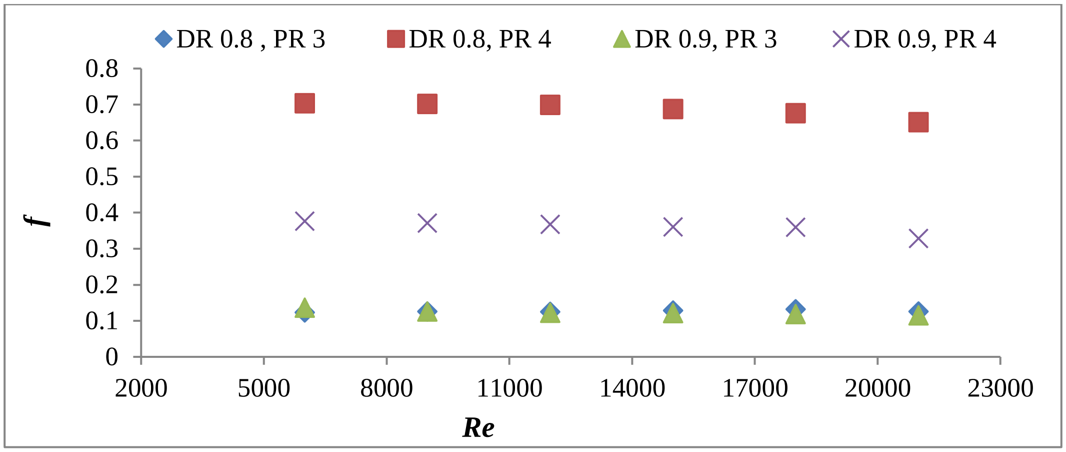

Figure 5 Effect of *f* with *Re* for CRWHS

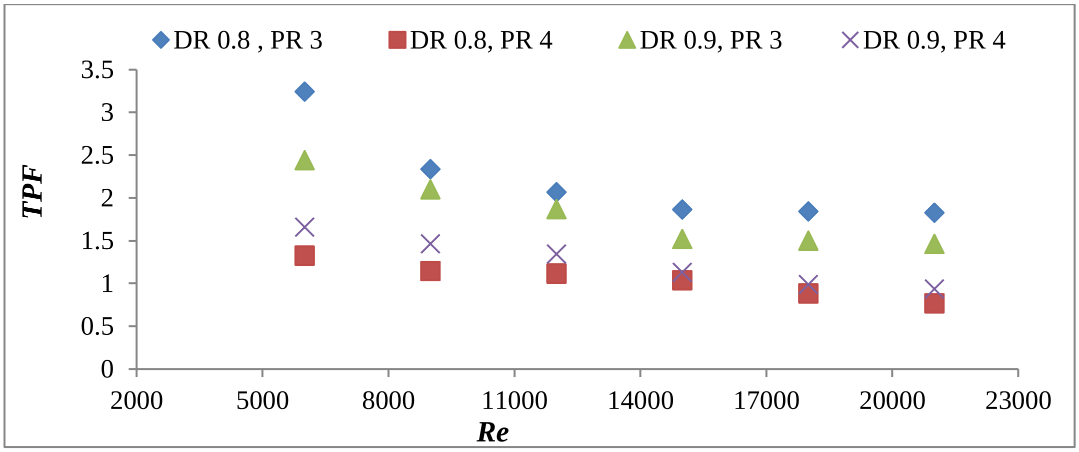

Figure 6 Effect of *TPF* with *Re* for CRWHS

NUMERICAL SIMULATION

Ansys 16.0 has been used for computational analysis of this work. For simulation, 1.5m length of the test section is made in which inserts of PR 3 and 4 are kept at DR 0.8 and 0.9. In the test section wall 1000 W/m^2 constant heat flux density is provided. For solving general equations pressure based solver are used. According to solution procedure of algorithm, they are classified into 2 parts- pressure based segregated algorithm and pressure based coupled algorithm. In pressure based segregated algorithm governing equations are solved well defined sequence each governing equation is solved sequentially. In pressure based coupled algorithm, continuity and momentum equations are solved simultaneously. The outlet temperature, wall mean temperature and the pressure difference between inlet and outlet are determined. For all variables the solution is converged. Results are calculated after the solution is converged to the 10^{-6}. The following equations are used during investigation:

Continuity Equation is taken as:

$$\left({\partial u_i}/{\partial x_i}\right)(\rho) = 0 \tag{11}$$

Momentum Equation is given by:

$$\left({\partial \rho}/{\partial (x_j)}\right)(u_i u_j) = {\partial}/{\partial (x_j)}\left[\left({\mu \partial u_i}/{\partial (x_j)}\right) + \left({\mu \partial u_j}/{\partial (x_i)}\right)\right] - {\partial p}/{\partial (x_i)} \tag{12}$$

Energy Equation:

$$\left({\partial u_j}/{\partial (x_j)}\right)(pc_p T) = \left({\partial}/{\partial (x_j)}\right)\left[k\left({\partial T}/{\partial (x_j)}\right)\right] \tag{13}$$

For the turbulence model k-ε equation is used.

k-Equation:

$$\rho\left[\bar{u}\left({\partial k}/{\partial x}\right) + \bar{v}\left({\partial k}/{\partial r}\right)\right] = \left({\partial}/{\partial x}\right)\left[\mu_1\left({\partial k}/{\partial x}\right) + \left({\mu_t}/{\sigma_k}\right)\left({\partial k}/{\partial x}\right)\right] + \left({\partial}/{r\partial r}\right)\left[(r\mu_1)\left({\partial k}/{\partial r}\right) + r\left({\mu_t}/{\sigma_k}\right)\left({\partial k}/{\partial r}\right)\right] - \rho\epsilon + \rho G \tag{14}$$

Where G is given by-

$$G = \mu_t\left[\left\{\left({\partial \bar{u}}/{\partial (r)}\right) + \left({\partial \bar{v}}/{\partial (x)}\right)\right\}^2 + 2\left\{\left({\bar{v}}/{(r)}\right)^2 + \left({\partial \bar{v}}/{\partial (r)}\right)^2 + \left({\partial \bar{u}}/{\partial (x)}\right)^2\right\}\right] \tag{15}$$

ε-Equation:

$$\rho\left[\bar{u}\left({\partial\varepsilon}/{\partial x}\right)+\bar{v}\left({\partial\varepsilon}/{\partial r}\right)\right]=\left({\partial}/{\partial x}\right)\left[\mu_1\left({\partial\varepsilon}/{\partial x}\right)+\left({\mu_1}/{\sigma_\varepsilon}\right)\left({\partial\varepsilon}/{\partial x}\right)\right]+\left({\partial}/{r\partial r}\right)\left[(r\mu_1)\left({\partial\varepsilon}/{\partial r}\right)+\left({\mu_1}/{\sigma_\varepsilon}\right)\left({\partial\varepsilon}/{\partial r}\right)\right]+GC_{s1}\left({\varepsilon}/{k}\right)-C_{s2}\left({\varepsilon^2}/{k}\right) \quad (16)$$

“Design modeler” was used for the designing the fluid domain and after that it further divided into the subparts using “mesh” cell. Figure 7 shows the meshing of fluid domain. Table 1 presents Grid independence test (GIT) in which change in number of nodes creates difference in the obtain results. Smoothing medium with relevance center was used during simulation. The deviation is limited to ±0.4% in *Nu* and ± 0.1% in *f*, after 8, 02,572 elements. Therefore for less time required to simulate for solving the computational problem 8,02,572 elements were selected for further analysis of results.

Table 1: GIT for the investigation

Relevance center	**Smoothing**	**Nodes**	***[Nu]***	$\left\lvert\frac{(Nu^{i+1})-(Nu^{i})}{(Nu^{i+1})}\right\rvert$	***[f]***	$\left\lvert\frac{(f^{i+1})-(f^{i})}{(f^{i+1})}\right\rvert$
Coarse	Low	340642	142.74	-	0.3176	-
Coarse	Medium	342044	137.02	4.80239	0.3055	5.75658
Medium	Low	798546	130.4	5.81132	0.3023	1.96334
Medium	Medium	802572	129.93	0.64821	0.3025	0.30852
Fine	Low	1574959	129.75	0.40422	0.3027	0.30838
Fine	High	1584515	129.71	0.28602	0.3026	0.25338

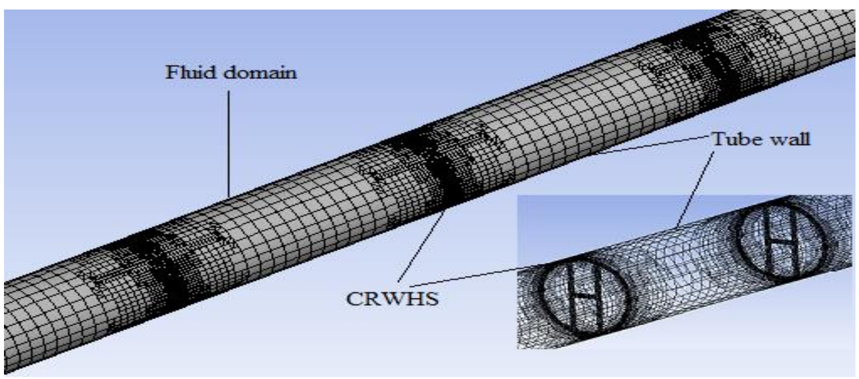

Figure 7 Meshing of fluid domain

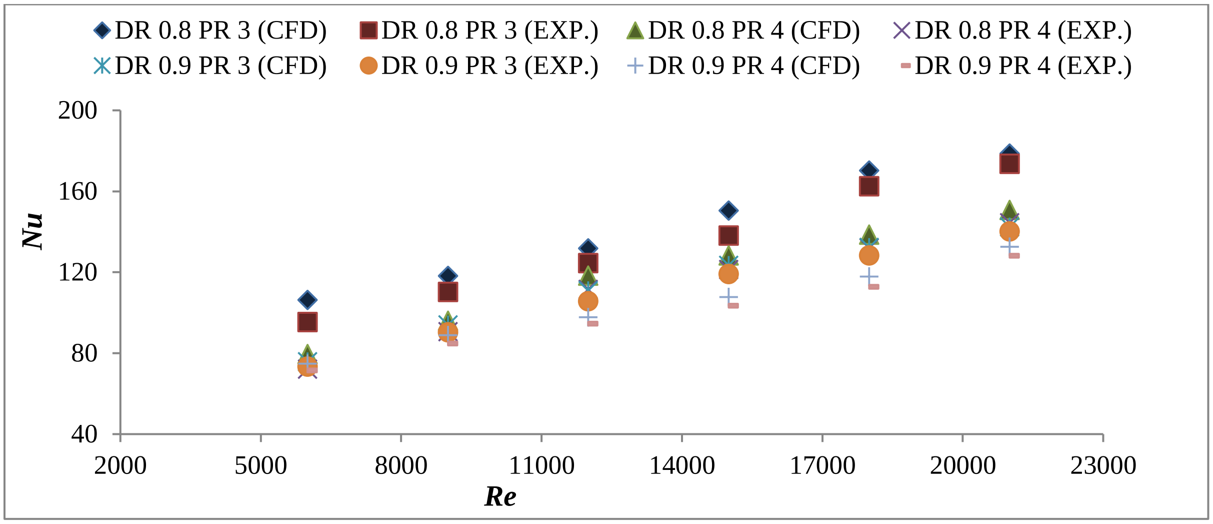

Figure 8 Comparison of *Nu* of computationally and experimentally for CRWHS

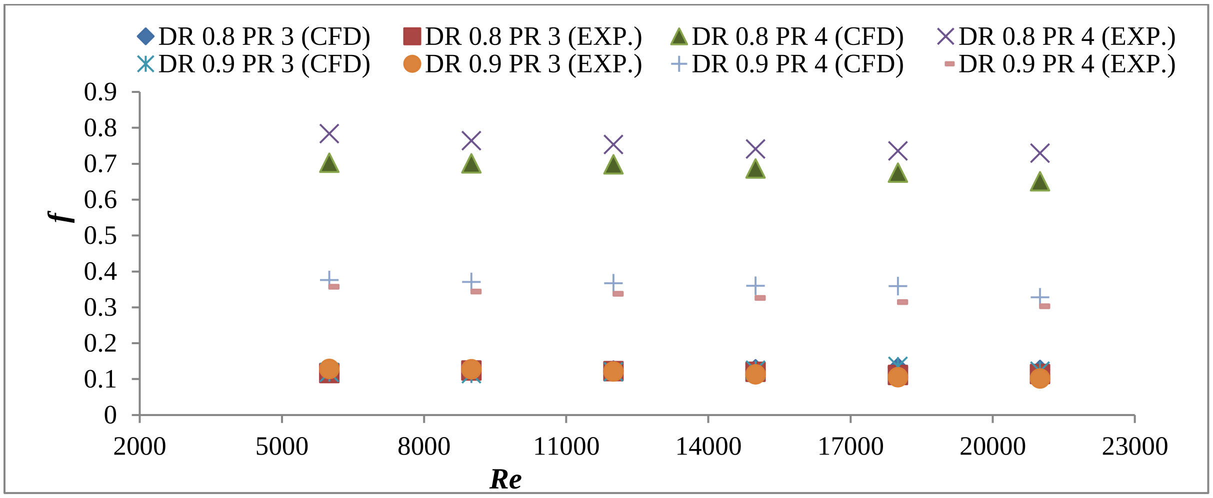

Figure 9 Comparison of *f* calculated computationally and experimentally for CRWHS

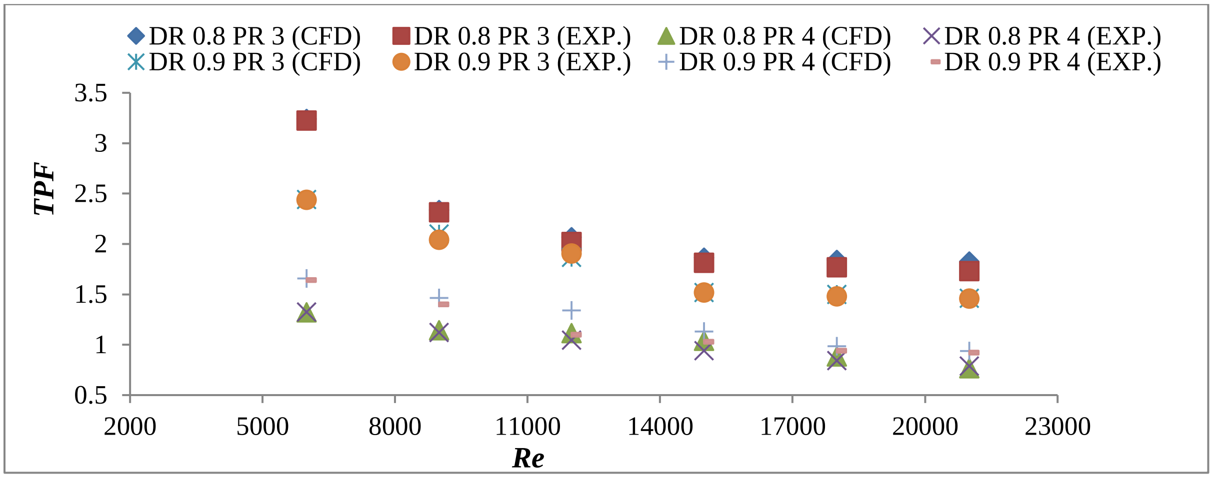

Figure 10 Comparison of *TPF* calculated computationally and experimentally for CRWHSThe comparative study of experimental and computational results for *Nu*, *f* and *TPF* using CRWHS inserts are presented in figures 8, 9 & 10 respectively. The result showed the maximum deviations are limited to ±6.3% in *Nu*, ±7.8% in *f* and 3.6% in *TPF*. Deviation occurs because during experimentation the condition of the room changes and for the computational conditions solver is used. Figure 11 shows the fluid flow profile inside the tube in which inserts restricts the fluid flow path and creates turbulence inside the main section that helps to moderate the formation of thermal layer inside the testing tube that lead to create intermixing the flow and which resulted the enhancement in heat transfer rate.

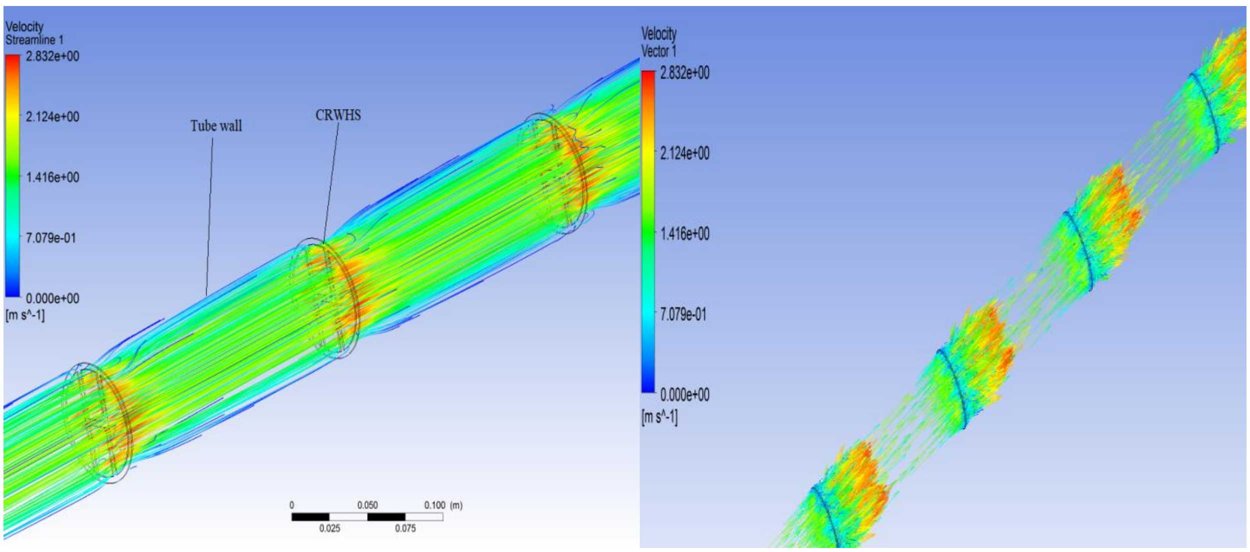

Figure 11 Streamline, vector representation of fluid flow inside the tube

Comparison with previous published works

To compare the results of CRWHS inserts with previous works in which they used different geometry of inserts in circular tube heat exchanger are presented in figure 12. The geometries used by researchers, (Eiamsa-ard et al., 2011) delta-wing with double-sided tape insert, (Vashishtha et al., 2016) multiple inserts, (Kumar et al., 2016) circular rings, (Gautam et al., 2018) perforation in triple wing vortex generator, (Promvonge et al., 2014) inclined vortex rings and (Bhuyia et al., 2014) double counter twisted tape inserts. From the figure it is noted that the CRWHS inserts gives higher TPF from the previous published work.

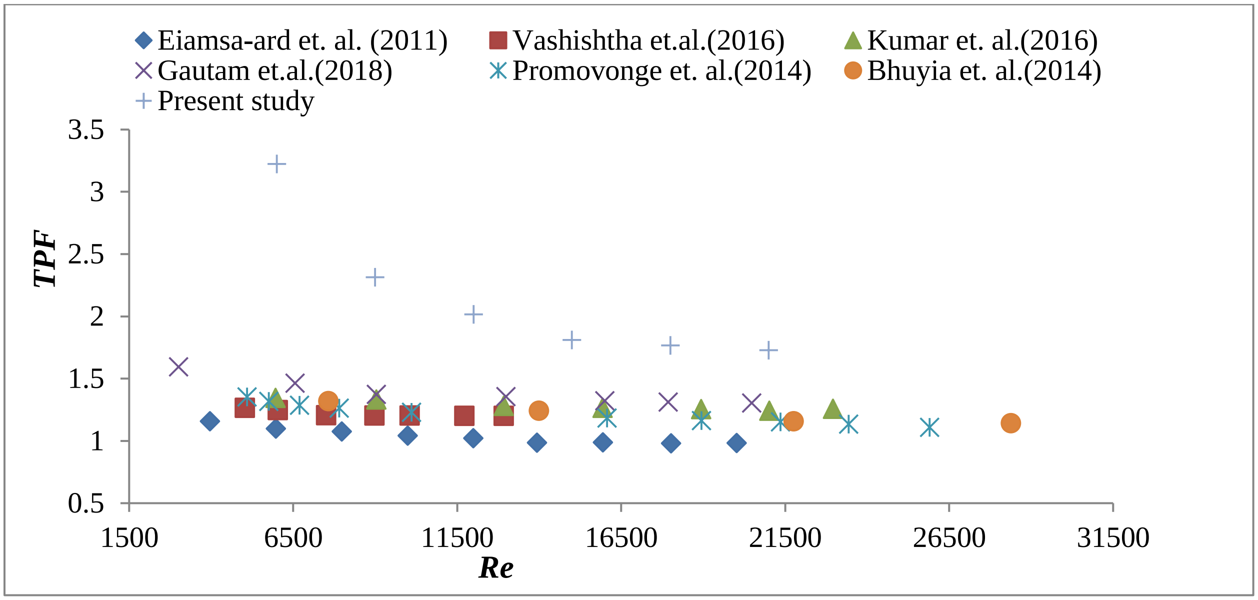

Figure 12 Comparison of CRWHS with previous published work

CONCLUSION

Computational and experimental analysis of fluid flow characteristics and heat transfer of a tube heat exchanger using CRWHS insert, the flow parameters shows major effect on thermal performance, heat transfer and friction factor. TPF is found maximum for minimum velocity i.e. low value of Reynolds number. With CRWHS inserts heat transfer rate is 4.56 times augmentation over the smooth tube for *Re*=6000. The value of friction factor 0.7033 is maximum for DR 0.8 and PR 4. Maximum achieved *TPF* is 3.24 for diameter ratio 0.8 and pitch ratio 3.Comparative study of experimental with computational gives a limited deviation among the results. Performance of CRWHS insert is found significantly high as compared to previous researchers work.

REFERENCES

Kongkaitpaiboon Vichan, Nanan Kwanchai, Eiamsa-ard Smith. 2010. Experimental investigation of pressure loss and convective heat transfer in a round tube fitted with circular-ring turbulators, International Communications in Heat and Mass Transfer 37: 568–574.

Eiamsa-ard Smith, Kongkaitpaiboon Vichan, Nanan Kwanchai. 2013. Thermo hydraulics of turbulent flow through heat exchanger tubes fitted with circular-rings and twisted tapes, Chinese Journal of chemical engineering, 21 (6) 585-593.

Akcayoglu Azize, 2011. Flow past confined delta-wing type vortex generators, Experimental Thermal and Fluid Science 35: 112–120.

Eiamsa-ard S, Promvonge P. 2011. Influence Delta-wing of Double-sided Tape Insert with Alternate-axes on Flow and Heat Transfer Characteristics in a Heat Exchanger Tube, fluid flow and transport phenomena, Chinese Journal of Chemical Engineering, 19: 410-423.

Khoshvaght-Aliabadi M., Sartipzadeh O., Alizadeh A. 2015. An experimental study on vortex-generator insert with different arrangements of delta-winglets, Energy xxx: 1e11.

Zhu J.D., Chen H. 2015. Numerical study of twisted tape inserts to enhanced heat transfer inside tube, Procedia Engineering 130: 256 – 262.

Vashishtha Chaitanya, Patil Anil Kumar, Kumar Manoj. 2016. Experimental investigation of heat transfer and pressure drop in a circular tube with multiple inserts, Applied Thermal Engineering 96: 117-129.

Alzahrani Salman, Usman Shoaib. 2019. CFD simulations of the effect of in-tube twisted tape design on heat transfer and pressure drop in natural circulation, Thermal Science and Engineering Progress, doi: https://doi.org/10.1016/j.tsep.2019.03.017.

Hong Y., Du J., Li Q., Xu T., Li W. 2019. Thermal-hydraulic performances in multiple twisted tapes inserted sinusoidal rib tube heat exchangers for exhaust gas heat recovery applications, Energy Conversion and Management 185: 271–290.

Gholamalizadeh E., Hosseini E., Jamanani M., Amiri A., Sare A., Alimoradi A. 2019. Study of intensification of the heat transfer in helically coiled tube heat exchanger via coiled wire inserts, International Journal of Thermal Sciences, 141: 72-83.

Sheikholeslami M., Gorji-Bandpy M., Ganji D. 2016. Effect of discontinuous helical turbulators on heat transfer characteristics of double pipe water to air heat exchanger, Energy Conversion and Management 118 (2016) 75–87.

Kongkaitpaiboon V., Nanan K., Eiamsa-ard S. 2010. Experimental investigation of convective heat transfer and pressure loss in a round tube fitted with circular-ring turbulators, International Communications in Heat and Mass Transfer 37: 568–574.

Kumar A., Chamoli S., Kumar M. 2016. Experimental investigation on thermal performance and fluid flow characteristics in heat exchanger tube with solid hollow circular disk inserts, Applied Thermal Engineering, 100: 227–236.

Singh S., Negi J., Bisht S., and Sah H. 2019. “Thermal performance and frictional losses study of solid hollow circular disc with rectangular wings in circular tube,” Heat Mass Transfer, vol. 55, pp. 2975–2986. DOI: 10.1007/ s00231-019-02631-z.

Zong Y., Bai D., Zhou M., Zhao L. 2019. Numerical studies on heat transfer enhancement by hollow-cross disk for cracking coils, Chemical Engineering & Processing: Process Intensification 135: 82–92.

Bartwal A., Gautam A., Kumar M., Mamgrulkar C., Chamoli S. 2018. Thermal performance intensification of a circular heat exchanger tube integrated with compound circular ring- metal wire net inserts, Chemical Engineering & Processing Process intensification, 124: 50-70.

Hameed V., Hussein M. 2017. Effect of new type of enhancement on inside and outside surface of the tube side in single pass heat Exchanger, Applied Thermal Engineering 122: 484-491.

Nagarajan P.K. and Sivashanmugam P. 2011. Heat Transfer Enhancement Studies in a Circular Tube Fitted with Right-Left Helical Inserts with Spacer, World Academy of Science, Engineering and Technology, International Journal of Mechanical and Mechatronics Engineering 5: 2091-2095.

Gururatana S., Skullong S. 2019. Experimental investigation of heat transfer in a tube heat exchanger with airfoil-shaped insert, Case Studies in Thermal Engineering, doi: https:// doi.org/10.1016/j.csite.

Sripattanapipat S., Tamna, Jayranaiwachira N., Promvonge P. 2016. Numerical heat transfer investigation in a heat exchanger tube with hexagonal conical-ring inserts, Energy Procedia, 100:522 – 525.

Gautam A., Pandey L., Singh S., 2018. Influence of perforated triple wing vortex generator on a turbulent flow through a circular tube, Volume 54, Issue 7, pp.2009-2021.

Promvonge P., Koolnapadol N., Pimsarn M., and Thianpong C., 2014. "Thermal performance enhancement in a heat exchanger tube fitted with inclined vortex rings," Appl. Therm. Eng., vol. 62, pp. 285–292, 2014. DOI: 10.1016/j.applthermaleng.2013.09.031.

Bhuiya M. M. K., Sayema A. S. M., Islam M., Chowdhury M. S. U., and Shahabuddine M., 2014. "Performance assessment in a heat exchanger tube fitted with double counter twisted tape inserts," Int. Commun. Heat Mass Transfer, vol. 50, pp. 25–33, 2014. DOI:10.1016/j.icheatmasstransfer.2013.11.005.

Webb R.L., Kim N.H., 2005. Principles of Enhanced Heat Transfer, second ed., Taylor& Francis Group, New York.